Applied Mathematical Modelling 40 (2016) 7182–7194

Contents lists available at ScienceDirect

Applied Mathematical Modelling

journal homepage: www.elsevier.com/locate/apm

An accurate fingerprint orientation modeling algorithm

Puneet Gupta [a,*], Phalguni Gupta [b]

[a] Department of Computer Science and Engineering, Indian Institute of Technology Kanpur, Kanpur 208016, India
[b] National Institute of Technical Teachers' Training and Research, Kolkata 700106, India

ARTICLE INFO

Article history:
Received 6 February 2015
Revised 2 January 2016
Accepted 9 March 2016
Available online 23 March 2016

Keywords:
Biometrics
Fingerprint orientation field estimation
Fingerprint orientation modeling
Variational based regularization

ABSTRACT

Orientation field (OF) plays a crucial role in singular point detection, fingerprint image enhancement, fingerprint matching, fingerprint indexing, fingerprint synthesis, fingerprint registration and fingerprint classification. Thus, an accurate OF estimation algorithm is proposed in this paper. It presents a novel OF regularization algorithm based on variational approach, which aims to preserve the genuine OF in the areas containing uniform flow and to accurately reconstruct the OF in bad quality areas. Estimated OF may be spurious in singular points close-by areas thus, it is further refined by weighted OF modeling based on Fourier basis. Experimental results are conducted on a publicly available database, FVC2004DB1A in terms of singular point detection and deviation in OF. It demonstrated that the proposed algorithm exhibit better performance that the state of the art algorithms.

1. Introduction

Orientation field (OF) is defined as a mapping function which maps set of observations to the interval of orientations [0, π) such that 0 is associated with π [1]. Tangent at each point of the vector field or OF gives the integral curve. OF is used in fingerprint analysis because integral curves of the OF can be used to represent the fingerprint ridge lines accurately [2].

Demand for better fingerprint based recognition system is increasing day by day because fingerprint can be easily collected in a user friendly manner and can assure universality, uniqueness and permanence [3]. The performance of fingerprint recognition systems is mainly restricted by the poor quality fingerprints which may be generated due to many reasons such as: (i) dirty, greasy, wounded or dry finger; (ii) creases or scars on the fingertip; (iii) environmental conditions like humidity or temperature [4]; (iv) dirt or latent print present on sensor [5]; and (v) smoothening of ridge-valley structure due to age or occupation [6].

Orientation field (OF) plays a crucial role in fingerprint enhancement, quality estimation, feature detection (like minutiae or singular points) and feature matching [7]. In fingerprint enhancement, the ridge-valley pattern is improved by contextual filtering techniques using OF [8,9]. Most of the fingerprint quality estimation algorithms are based on the intuition that there is uniform ridge-valley flow in case of good quality fingerprints [10]. Thus, OF provides a useful indication of fingerprint quality. Singular points are used as global feature in some of the system [11]. These are the points of discontinuity in OF [12]. Various global feature matching algorithms are based on fingerprint registration using OF [13]. Moreover, OF can also be used for fingerprint synthesis [14], fingerprint indexing [15], fingerprint classification [16] and template update [17].

* Corresponding author. Tel.: +91 9559754489; fax: +91 5122597579.
E-mail addresses: puneet@cse.iitk.ac.in, puneet@iitk.ac.in (P. Gupta), director@nitttrkol.ac.in (P. Gupta).

http://dx.doi.org/10.1016/j.apm.2016.03.009
S0307-904X(16)30134-2/

Since OF plays a crucial role in fingerprint based recognition system, this paper deals with the problem of estimating OF accurately.

There is almost a linear ridge-valley flow in the local area of a fingerprint, except for singular points close-by areas. Thus, local methods use neighborhoods for OF estimation. These are mainly categorized as: gradient-based algorithm [18]; filter-bank based algorithm [19]; and frequency based algorithm [20]. To estimate the OF at a pixel, squared gradients of its local neighborhood are averaged in the gradient based algorithm. In filter-bank based algorithm, OF is estimated using several directional filters. In frequency based algorithm, OF at a pixel is determined by Fourier analysis of its local neighborhood. Any local method gives spurious OF estimates for the areas near singular points because these areas have large curvature. In addition, it fails in the areas of bad quality fingerprints. Low pass filtering [21] can somewhat reduce the spurious OF estimates. But it is ineffective if local neighborhoods cannot provide adequate ridge-valley flow information which usually occurs if a fingerprint area has bad quality or it lies close to a singular point. Regularization approaches based on local neighborhood can accurately smoothen or reconstruct OF containing linear flow [22,23]. However, it also performs poorly for bad quality fingerprint images [24]. In learning based approaches, variability among the global orientation patterns is learned using a training set [25,26]. It does not require the existence of singular points. It aims to replace a fingerprint area by the most suitable pattern available in the training set. Such smoothening is useful in noisy areas and thus, it is found to be successful in latent fingerprint [24]. However, it slightly deteriorates the OF in good quality areas and thus, usually avoided for the fingerprints acquired from an acquisition device like optical sensor [27].

Global fingerprint structure can be used for OF estimation in such a way that OF in bad quality areas can be accurately interpolated. Since areas close to singular points have high curvature, modeled OF is spurious near such areas. Knowledge of singular points have been used in some global OF modeling algorithms [12,28,29]. But an accurate detection of singular point is a hard problem for bad quality fingerprints; thus these algorithms are not much useful. Problem of fingerprint OF modeling can also be expressed as a data fitting problem where OF obtained from a local method is fitted on some well defined basis functions. Optimization algorithms are applied to obtain the modeling parameters required for data fitting. The basis functions and the modeling parameters are used to reconstruct or model the OF. During modeling, OF estimates in [30] and [15] are treated equally by the data fitting algorithms. The modeled OF can be refined by singular point detection [31]. The data fitting algorithms can generate spurious modeled OF estimates for bad quality areas and for the areas near to singular points because equal weights are given to each local OF estimates during modeling. It would be appropriate if areas consisting of uniform ridge-valley flow are given more importance as compared to the areas having bad quality. This is leveraged by weighted OF modeling algorithms which aim to reconstruct OF in bad quality areas using OF available in good quality areas [27,32–34]. In algorithm [32], weights are assigned based on foreground and background pixels. Even though it exhibits better performance than algorithms [30] and [15], it gives spurious modeled OF estimates in bad quality areas or singular points close-by areas. Linear ridge-valley flow can be used to assign the weights for evading the problems of bad quality [27,33] but it assigns low weights in the areas near singular points. Weights can also be assigned based on probable location of singular points [34] but it is inappropriate when singular points are absent (like in an arch type fingerprint) or spurious singular points are obtained due to bad quality fingerprint areas. It can be seen that the success of data-fitting based global OF modeling mainly relies on accurate local OF estimates and proper weight assignment.

As an epitome, local methods give spurious OF estimates in areas containing bad quality or large curvature due to singular points. Global methods based on singular point detection show poor performance for bad quality fingerprints where singular points cannot be determined accurately. In contrast, global methods based on data fitting do not detect singular points but preserve OF near singular points and accurately reconstruct the OF for bad quality areas. Performance of these algorithms can be enhanced using appropriate weights and proper local OF estimates. This paper proposes an OF estimation algorithm which uses symmetric filter based weight estimation, local regularization and weighted OF modeling. The weights are assigned based on uniformity in ridge-valley flow. The proposed local regularization aims to preserve the genuine OF in the areas which contain uniform flow and to reconstruct the OF in bad quality areas having linear flow. But it cannot reconstruct OF accurately in the singular points close-by areas having bad quality. Thus, weighted OF modeling based on data-fitting algorithm is subsequently applied. The contributions of this paper are that it proposes a novel OF regularization algorithm and it commences the use of both regularization and data-fitting algorithms for better OF modeling. The proposed algorithm does not require any prior knowledge of singular points and it is found to be better than state of the art algorithms.

This paper is organized as follows. The proposed orientation field modeling algorithm is presented in the next section. Experimental results are analyzed in Section 3. Conclusions are given in the last section.

2. Proposed algorithm

The flow-graph of the proposed fingerprint OF estimation algorithm is shown in Fig. 1. It consists of four stages. In the first stage, fingerprint OF is extracted using a gradient based local algorithm. It may be spurious for bad quality areas and singular points close-by areas. OF in uniform flow areas should be preserved while OF in non-uniform flow areas should be interpolated using local neighbors and global topology of the fingerprint for accurate OF estimation. Therefore, in the next stage, weights are assigned according to the uniformity in ridge-valley flow. In the third stage, a regularization algorithm is proposed to smoothen adaptively the OF using local neighbors. Eventually, the smoothen OF is further refined using a weighted OF modeling algorithm.

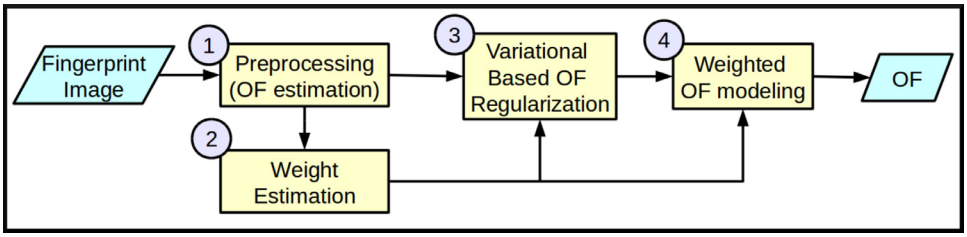

Fig. 1. FlowGraph of the Proposed System.

2.1. Preprocessing

In this section, pixel-wise OF of fingerprint is estimated using a local method which has been proposed in [8]. A fingerprint is composed of foreground and background blocks that have high and low variances respectively. Typically, blocks containing fingerprint, i.e., foreground blocks have high variance due to alternate ridge-valley present in the blocks. However, background blocks containing smooth non-varying intensity patterns have low variance. By analyzing the variance, background blocks are detected and subsequently removed. Resultant image is normalized to zero mean and unit variance [35]. Least mean square is applied on the normalized image to estimate the pixel-wise OF. Let θ denote the OF of a block centered at pixel (i, j). Then,

$$\theta(i,j) = \frac{1}{2}\tan^{-1}\left(\frac{\sum_{u=i-\frac{w}{2}}^{i+\frac{w}{2}}\sum_{v=j-\frac{w}{2}}^{j+\frac{w}{2}} 2G_x(i,j)G_y(i,j)}{\sum_{u=i-\frac{w}{2}}^{i+\frac{w}{2}}\sum_{v=j-\frac{w}{2}}^{j+\frac{w}{2}}(G_x^2(i,j)-G_y^2 i,j))}\right), \tag{1}$$

where w is the block size and G_x and G_y are the gradients in x and y direction respectively that are evaluated by applying Sobel operator on the normalized image. OF is estimated at each pixel using a block centered at that pixel. OF is further smoothened by a low pass Gaussian filter to eliminate some noise artifacts.

2.2. Weights estimation

In this section, weights required in OF modeling are estimated such that: (i) high values are assigned to singular points close-by areas containing uniform ridge-valley flow; (ii) high values are assigned to the uniform and linear ridge-valley flow areas; and (iii) low values are assigned to dry and wet fingerprint areas containing non-uniform ridge-valley flow. Parabolic symmetric filters can measure the uniformity in ridge-valley flow for the areas near singular points [36]. So symmetric filters have been used in this paper for weight estimation. Algorithms relying on the strength of OF like Gabor filter based approach and orientation certainty level assign low values to singular points close-by areas due to high curvature and hence, avoided [10]. Primarily, a symmetric filter works as follow. A filter representing a symmetric shape pattern has been formed using the domain knowledge. Filter response is obtained by convolving the filter with the orientation tensor containing the edge information. It gives the similarity between the local orientations and the filter.

A fingerprint mainly contains three type of uniform ridge-valley flows, viz., linear flow, flow near core points and flow near delta points which can be modeled using symmetric filters of order −1, 0 and 1 [37]. Let h_j denotes the symmetric filter corresponding to order j (where j = −1, 0 , 1). It is obtained at a pixel location (x, y) using:

$$h_j(x,y) = \begin{cases} (x+iy)^j \cdot g(x,y) & if\ \ j \geq 0, \\ (x-iy)^{|j|} \cdot g(x,y) & otherwise, \end{cases} \tag{2}$$

such that g follows a 2D Gaussian distribution. Orientation tensor, z, of a fingerprint is given by:

$$z = \cos(2\times\theta) + i\sin(2\times\theta). \tag{3}$$

Let S_j represents the filter response obtained by convolving h_j with z. That is,

$$S_j = \frac{\langle z, h_j\rangle}{\langle |z|, h_0\rangle}. \tag{4}$$

In Eq. (4), normalization is applied along with convolution to restrict S_j between 0 and 1 [38]. Let S_0, S_1 and S_{-1} denote the filter responses corresponding to h_0, h_1 or h_{-1}, respectively [37]. These are used to measure the uniformity in various kinds of ridge-valley flow. It is observed that a fingerprint area must resemble to a symmetric filter and if it resembles to more than one symmetric filter then it has non-uniform ridge-valley flow occurred due to noise or blur. For assigning low values to the filter responses in case of non-uniform ridge-valley flow areas, filter responses are modified using

$$\hat{S}_j = S_j \prod_{k\in\{-1,0,1\}\setminus j} (1-|S_k|), \tag{5}$$

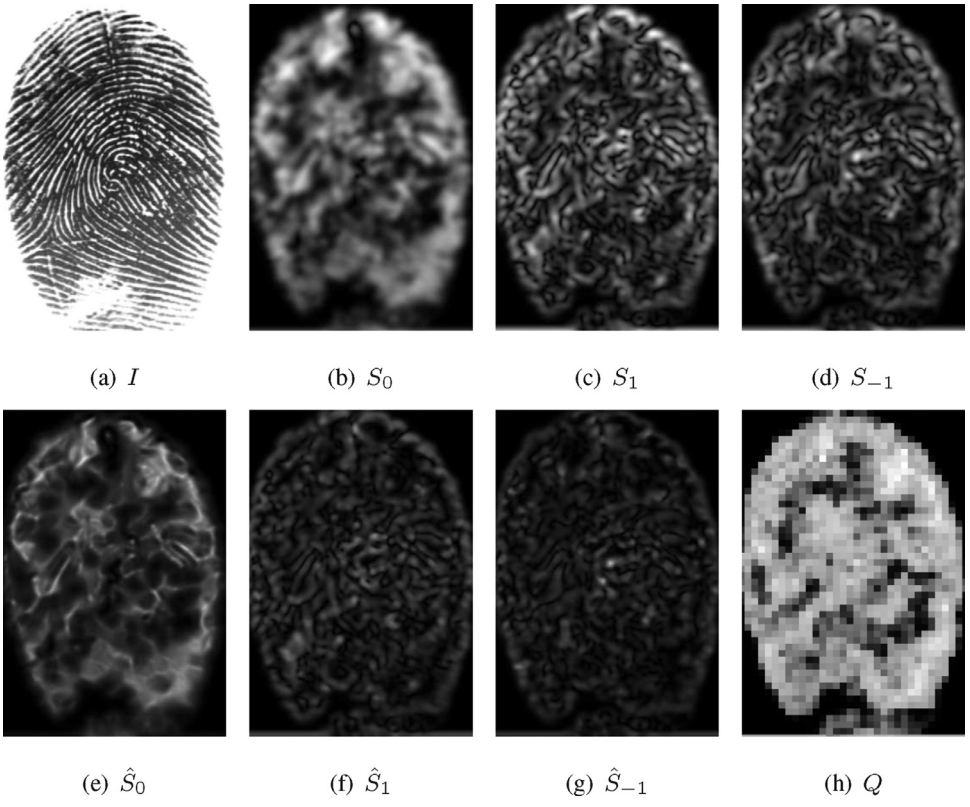

Fig. 2. Example of Weight Estimation using Symmetric Filter.

where $\hat{S}_j$ represents the modified filter response corresponding to S_j and \ represent the set difference operation [39]. Modified filter responses for $j = \{-1, 0, 1\}$ are consolidated using

$$Q = \hat{S}_{-1} + \hat{S}_0 + \hat{S}_1. \tag{6}$$

Block-wise weight estimates are used to remove noise in Q. Q is divided into non-overlapping blocks and mean value of a block represent weight of the block. Weight of a block is subsequently replicated at each pixel of the block to obtain pixel-wise weight estimates. Steps required to obtain the weights, Q, are given in Algorithm 1. For visualization, consider

Algorithm 1 FingerprintQuality(θ).

Require: θ represent the orientation field.
Ensure: Q contains the fingerprint quality.
1: Create symmetric filters h_0, h_1 and h_{-1} using Equation (2) for n = 0,1 and -1.
2: Find orientation tensor, z using Equation (3).
3: Symmetric descriptors S_0, S_1 and S_{-1} are obtained corresponding to h_0, h_1 and h_{-1} using Equation (4).
4: **for** each pixel (x, y) in I **do**
5: Obtain modified symmetric descriptors at each pixel ($\hat{S}_0(x, y)$, $\hat{S}_1(x, y)$, $\hat{S}_{-1}(x, y)$) using Equation (5).
6: $Q(x, y) = \hat{S}_0(x, y) + \hat{S}_1(x, y) + \hat{S}_{-1}(x, y)$
7: **end for**
8: Divide Q into non overlapping blocks.
9: **for** each block k in Q **do**
10: Find the mean of k and replicate it at each pixel of the block k.
11: **end for**
12: **return** (Q)

Fig. 2 depicting an example of the proposed weight estimation algorithm. It can be seen from Fig. 2(h) that low weights are assigned to non-uniform ridge-valley flow areas and high weights are assigned to uniform ridge-valley flow areas.

2.3. OF regularization

A local regularization algorithm is presented in this section which aims to: i) preserve the genuine OF in the areas having uniform flow irrespective of curvature; and ii) reconstruct the spurious OF in bad quality areas using local neighborhoods. Let T represent the modeled OF. It should be similar to θ for uniform flow areas. Thus, similarity between T and θ is minimized to maintain such a data fidelity constraint [40]. The similarity is given by the weighted sum of squared errors where weights are assigned based on uniformity in ridge-valley flow. Thus,

$$\hat{F}(T) = \int_x \int_y Q(x,y)(\theta(x,y) - T(x,y))^2 \mathrm{d}x\ \mathrm{d}y, \tag{7}$$

needs to be minimized to satisfy the data fidelity constraint. In Eq. (7), (x, y) denotes a pixel location. Generally, there is uniform flow in a fingerprint except at singular point locations. Therefore, T should satisfy the smoothness constraint given by

$$G(T) = \int_x \int_y \left|\bigtriangledown T(x,y)\right|^2 \mathrm{d}x\ \mathrm{d}y, \tag{8}$$

where

$$\bigtriangledown T(x,y) = \frac{\partial T(x,y)}{\partial x} + \frac{\partial T(x,y)}{\partial y}. \tag{9}$$

For accurate estimation of T, both $\hat{F}(T)$ and $G(T)$ should be minimized but these functions are competitive. In other words, $G(T)$ is minimized when T is constant but it clearly leads to high value of $\hat{F}(T)$. Likewise, minimization of $\hat{F}(T)$ requires that θ and T are pixel-wise equal, which results in high value of $G(T)$ near noise pixels. Hence, a combined function, $P(T, \alpha)$, is formed which requires an adaptive parameter α to control the impact of $\hat{F}(T)$ and $G(T)$. It is given by:

$$P(T,\alpha) = \frac{1}{2}\left(\sqrt{1-\alpha^2}\hat{F}(T) + \alpha G(T)\right). \tag{10}$$

Such a non-linear combination of $\hat{F}(T)$ and $G(T)$ is chosen because it automatically allows the variational minimax optimization to obtain the global optimal solution of T and α. Due to this combination, $P(T, \alpha)$ has concave–convex behavior, i.e., it is strictly convex in terms of T and strictly concave in terms of α [41]. This creates a unique saddle point which can be determined using variational approach. It is observed that minimization of $P(T, \alpha)$ satisfies the requirement of effective OF regularization in following ways:

1. For the areas containing uniform and linear ridge-valley flow, both $\hat{F}(T)$ and $G(T)$ can be simultaneously minimized by preserving the genuine OF.
2. For the uniform flow areas containing high curvature due to singular points, $\hat{F}(T)$ and $G(T)$ are competitive. Since high values of Q are assigned to such areas due to uniformity, $\hat{F}(T)$ has high value. Hence in these areas, genuine OF is preserved with little smoothening due to $G(T)$, which can deviate the singular points from their actual locations.
3. In contrast, low values of Q are assigned to non-uniform flow areas that results in low value of $\hat{F}(T)$. Thus, $P(T, \alpha)$ can be minimized by minimizing $G(T)$ which requires OF reconstruction using local neighborhoods. Such reconstructed OF is accurate in the areas having non-uniform and linear flow. But it is inaccurate in non-linear flow areas having large curvature and leads to deviation of singular point locations.

If $\hat{F}$ plays a dominant role in P then spurious OF in areas having non-uniform flow remains intact in T. In contrast, if G plays a dominant role in P then uniform flow near high curvature areas is lost. T can be computed by minimax solution of P, i.e., $P(T, \alpha)$ is minimized with respect to T while maximized with respect to α, that is,

$$\hat{T} = arg \max_{\alpha} \min_{T} P(T,\alpha), \tag{11}$$

where $\hat{T}$ denotes the estimated modeled OF. Inner and outer optimizations can be interchanged [42] in the present scenario because: i) $P(T, \alpha)$ contains a saddle point; and ii) T and α are compact sets. Thus, Eq. (11) can be rewritten as

$$\hat{T} = arg \min_{T} \max_{\alpha} P(T,\alpha), \tag{12}$$

which can be solved using variational minimax optimization.

Steps required for the proposed variational minimax optimization are given in Algorithm 2. T is initially set to θ, and it is iteratively refined for better estimates. In the first iteration, $P(T, \alpha)$ is maximized with respect to α and subsequently minimized with respect to T. Value of α that maximizes $P(T, \alpha)$ is obtained by differentiating $P(T, \alpha)$ in terms of α and equating to zero, i.e.,

$$\frac{\partial P(T,\alpha)}{\partial \alpha} = \frac{-\alpha}{\sqrt{1-\alpha^2}}\hat{F}(T) + G(T) = 0. \tag{13}$$

Algorithm 2 *OF_Variational_Modelling*(Q, θ).

Require: Q and θ storing uniformity in ridge-valley flow and OF respectively.
Ensure: Return T containing modelled OF.

$\bar{\alpha} = 0$
$T = \theta$
for $t = 1$ to 10 **do**
  $\alpha_1 = \bar{\alpha}$
  $\hat{F}(T) = \int_x \int_y Q(x,y)(\theta(x,y) - T(x,y))^2 \mathrm{d}x\ \mathrm{d}y$
  $G(T) = G(T) = \int_x \int_y \left| \frac{\partial T(x,y)}{\partial x} + \frac{\partial T(x,y)}{\partial y} \right|^2 \mathrm{d}x\ \mathrm{d}y$
  $\bar{\alpha} = \frac{G(T)}{\sqrt{(\hat{F}(T))^2 + (G(T))^2}}$
  At each pixel (i, j), evaluate $T_{i,j}^{new} = T_{i,j} + \tau\sqrt{1-\bar{\alpha}^2}\left(Q_{i,j}\left(\theta_{i,j} - T_{i,j}\right)\right) + \tau\bar{\alpha}\left(T_{i+1,j} + T_{i-1,j} + T_{i,j+1} + T_{i,j-1} - 4T_{i,j}\right)$
  $T = T^{new}$
  if $\alpha_1 - \bar{\alpha} < \epsilon$ **then**
    break // *This will break FOR loop*
  end if
end for
return T

Let $\bar{\alpha}$ denotes the value of α which maximizes $P(T, \alpha)$. It is given by

$$\bar{\alpha} = \frac{G(T)}{\sqrt{(\hat{F}(T))^2 + (G(T))^2}}. \tag{14}$$

Subsequently, function $P(T, \bar{\alpha})$ is minimized to obtain T using gradient descent. For simplicity, consider

$$P(T, \bar{\alpha}) = \int_x \int_y \Psi(T, T_x, T_y)\mathrm{d}x\ \mathrm{d}y, \tag{15}$$

where

$$\begin{aligned}\Psi(T, T_x, T_y) =& \sqrt{1-\bar{\alpha}^2}\left(Q(x,y)(\theta(x,y) - T(x,y))^2\right) \\ &+ \bar{\alpha}\left(|T_x(x,y) + T_y(x,y)|^2\right),\end{aligned} \tag{16}$$

while $T_x(x, y)$ and $T_y(x, y)$ are given by

$$T_x(x,y) = \frac{\partial T(x,y)}{\partial x}, \tag{17}$$

$$T_y(x,y) = \frac{\partial T(x,y)}{\partial y}. \tag{18}$$

Assume that modeled OF, T, is perturbed by a function, $h(x, y)$, whose first and second derivatives are continuous in the image domain. After transforming function $P(T, \bar{\alpha})$ into another function $P(T + h, \bar{\alpha})$ using h, variations are introduced in $P(T, \bar{\alpha})$ that can be estimated using Euler conditions. Let $\delta(P(T, \bar{\alpha}))$ represent the introduced variations that is given by

$$\delta(P(T,\bar{\alpha})) = \int_x \int_y \left(\frac{\partial \Psi}{\partial T} + \frac{\partial}{\partial x}\left(\frac{\partial \Psi}{\partial T_x}\right) + \frac{\partial}{\partial y}\left(\frac{\partial \Psi}{\partial T_y}\right)\right) h(x,y)\mathrm{d}x\mathrm{d}y, \tag{19}$$

where

$$\frac{\partial \Psi}{\partial T} = -\sqrt{1-\bar{\alpha}^2}(Q(x,y)(\theta(x,y) - T(x,y))), \tag{20}$$

$$\frac{\partial}{\partial x}\left(\frac{\partial \Psi}{\partial T_x}\right) = \frac{\partial}{\partial x}\left(\bar{\alpha}\frac{\partial T}{\partial x}\right) = \bar{\alpha}\frac{\partial^2 T}{\partial x^2}, \tag{21}$$

$$\frac{\partial}{\partial y}\left(\frac{\partial \Psi}{\partial T_y}\right) = \frac{\partial}{\partial y}\left(\bar{\alpha}\frac{\partial T}{\partial y}\right) = \bar{\alpha}\frac{\partial^2 T}{\partial y^2}. \tag{22}$$

Using the gradient descent technique, change in T, T_Δ, is given by

$$T_\Delta = -\left(\frac{\partial \Psi}{\partial T} + \frac{\partial}{\partial x}\left(\frac{\partial \Psi}{\partial T_x}\right) + \frac{\partial}{\partial y}\left(\frac{\partial \Psi}{\partial T_y}\right)\right). \tag{23}$$

Hence,

$$T_\Delta = \sqrt{1-\bar{\alpha}^2}(Q(x,y)(\theta(x,y)-T(x,y))) + \bar{\alpha}\left(\frac{\partial^2 T}{\partial x^2}+\frac{\partial^2 T}{\partial y^2}\right),$$

$$= \sqrt{1-\bar{\alpha}^2}(Q(x,y)(\theta(x,y)-T(x,y))) + \bar{\alpha}\overset{2}{\nabla}T(x,y). \tag{24}$$

Therefore, T is refined by

$$T = T + \tau T_\Delta, \tag{25}$$

where τ denotes the step-size. $\hat{F}(T)$ and $G(T)$ are refined using refined modeled OF, T. In next iteration, $\bar{\alpha}$ is evaluated using refined $\hat{F}(T)$ and $G(T)$ and it is used to subsequently refine T, $\hat{F}(T)$ and $G(T)$. Such an iterative refinement continues till the number of iterations exceeds a predetermined threshold or convergence condition is attained. If the difference between two successive $\bar{\alpha}$ is less than a threshold, ϵ then convergence condition is attained.

2.3.1. Numerical implementation

Generally, a 2D heat equation is represented by

$$\frac{\partial u}{\partial t} = c\left(\frac{\partial^2 u}{\partial x^2}+\frac{\partial^2 u}{\partial y^2}\right), \tag{26}$$

where function u depends on variables x, y and t and constant c. Finite difference method can be used to solve this heat equation [43]. It can be seen that Eq. 24 is a heat equation [44] with source term, S_t given by

$$S_t = \sqrt{1-\bar{\alpha}^2}(Q(x,y)(\theta(x,y)-T(x,y))). \tag{27}$$

Hence, difference formula requiring discrete finite values can be used instead of continuous derivatives in Eq. 24, i.e.,

$$\left(\frac{\partial T(x,y)}{\partial x}\right)_t = T^t_{i+1,j} - T^t_{i,j}, \tag{28}$$

$$\left(\frac{\partial T(x,y)}{\partial y}\right)_t = T^t_{i,j+1} - T^t_{i,j}, \tag{29}$$

$$\left(\frac{\partial^2 T}{\partial x^2}\right)_t = T^t_{i+1,j} - 2T^t_{i,j} + T^t_{i-1,j}, \tag{30}$$

$$\left(\frac{\partial^2 T}{\partial y^2}\right)_t = T^t_{i,j+1} - 2T^t_{i,j} + T^t_{i,j-1}, \tag{31}$$

where (i, j) represents a pixel location and t denotes the number of iterations. Hence, Eq. 24 can also be given by:

$$T^{t+1}_{i,j} = T^t_{i,j} + \tau\sqrt{1-\bar{\alpha}^2}\left(Q_{i,j}\left(\theta_{i,j}-T^t_{i,j}\right)\right) + \tau\bar{\alpha}\left(T^t_{i+1,j}+T^t_{i-1,j}+T^t_{i,j+1}+T^t_{i,j-1}-4T^t_{i,j}\right). \tag{32}$$

2.4. Weighted OF modeling

All known regularization approaches for OF modeling are ineffective for the areas containing high curvature because they require ridge-valley flow of local neighborhoods, which is insufficient to reconstruct accurately the flow of large curvature areas. Even the proposed regularization slightly smoothens the flow in large curvature areas and thus, displacing the location of singular points. Thus in this paper, weighted OF modeling is applied after OF regularization for rectification. Sine and cosine component of squared OF are modeled using Fourier basis function [15]. Let Φ denote the basis matrix while A and B represent modeling coefficients required for cosine and sine components of squared OF. Parameters A and B are modeled by

$$\hat{A} = \arg_A \min \|(\mathbf{W}(\mathbf{G_{cos}} - \Phi A)\|^2, \tag{33}$$

$$\hat{B} = \arg_B \min \|(\mathbf{W}(\mathbf{G_{sin}} - \Phi B)\|^2, \tag{34}$$

where $\hat{A}$ and $\hat{B}$ are the estimated coefficients corresponding to A and B respectively. These are obtained by minimizing the sum of squared residuals using weighted least squares. In addition, $\mathbf{G_{cos}}$ and $\mathbf{G_{sin}}$ represent the cosine and sine components respectively while $\mathbf{W}$ is the matrix containing the uniformity measure. Parameters $\mathbf{G_{cos}}$, $\mathbf{G_{sin}}$ and $\mathbf{W}$ are the column vectors defined at each pixel location. For the regularized OF, T, of size $m \times n$, these parameters are given by:

$$\mathbf{G_{cos}} = [\cos(2T(0,0)) \quad \cos(2T(0,1)) \cdots \quad \cos(2T(m,n))]^T, \tag{35}$$

$$\mathbf{G_{sin}} = [\sin(2T(0,0)) \quad \sin(2T(0,1)) \cdots \quad \sin(2T(m,n))]^T, \tag{36}$$

$$\mathbf{W} = [Q(0,0) \quad Q(0,1) \cdots \quad Q(m,n)]^T. \tag{37}$$

Weighted modeled OF, $\bar{\theta}$, is given by

$$\bar{\theta}(x,y) = \frac{1}{2}\tan^{-1}\frac{\left(\phi^T(x,y)\hat{B}\right)}{\left(\phi^T(x,y)\hat{A}\right)}. \tag{38}$$

3. Experimental results

In this section, experimental results have been analyzed.

3.1. Parameter tuning

Several parameters are used in the proposed algorithm for obtaining accurate results. These are discussed below:

1. Parameters like block size and low pass filter used in local OF estimation have been fine tuned using the algorithms in [45–47]. Symmetric filters are constructed with the help of parameters given in algorithm [48].
2. Tuning of three parameters are required for regularized OF modeling. These are the step-size, ϵ required in convergence condition and the maximum number of iterations. Since step-size should be less than or equal to $\frac{1}{4}$ for faster convergence in gradient based algorithms [49], the step-size is set to $\frac{1}{4}$. ϵ should be as minimum as possible for better results and thus, it is given by the machine epsilon [50]. It is observed that the proposed OF regularization has fast convergence rate and thus usually the convergence condition is attained rather than exceeding the maximum number of iterations. But in a few cases, the difference between two successive $\bar{\alpha}$ is pretty small but greater than the minimum possible value, ϵ. and in these cases the algorithm can be iterated large number of times without giving sufficient improvement. Thus, the number of iterations is restricted for efficiency purpose while testing on a publicly available database FVC2004 DB1B [51] having 80 fingerprint images. FVC2004 DB1B is the training set corresponding to the test set FVC2004 DB1A. When the proposed OF regularization is applied on 80 images of FVC2004 DB1B database, it is observed that the convergence is attained in 73 images before 10 iterations while for the remaining 7 images the convergence is attained after 120 iterations. Moreover, small improvements are introduced in the remaining 7 images after 10 iterations and thus the maximum number of iterations is set to 10 to achieve the maximum accuracy.
3. Order of basis function, required in weighted orientation modeling is crucial because its small value smoothen the modeled OF in large curvature areas while its large value may cause the modeling of noises instead of smoothening. Order is set to be 6 as suggested in [27] to achieve the most accurate OF modeling for Fourier basis functions.

Fig. 3 shows some examples of the proposed OF modeling for qualitative comparison. It depicts that the proposed algorithm has accurately reconstructed the fingerprint OF. As discussed in [27], singular point detection and OF deviation have been used to evaluate the performance of modeled OF.

3.2. Singular point detection

The performance of OF modeling can be analyzed by correct detection and accurate localization of singular points because of the following reasons:

1. If a singular point is correctly detected and localized, then it indicates that the modeled OF and actual OF in the local neighborhood of the singular point are similar. In such a case, genuine OF is preserved in singular point close-by areas containing uniform flow or it is accurately interpolated in singular point close-by areas containing non-uniform flow.
2. Likewise, if genuine singular points are accurately detected with low localization error, then it indicates that the modeled OF in the local neighborhood of the singular point deviates from the actual OF.
3. Existence of spurious singular points indicates that modeled OF and actual OF in the local neighborhood of the singular point are highly dissimilar. Such a case is applicable when bad quality areas containing linear flow are incorrectly modeled.

The publicly available database FVC2004 DB1A [51] has been used to analyze the performance of the proposed algorithm. It contains 800 fingerprint images acquired from an optical sensor under uncontrolled environment that results in bad quality fingerprints [52]. Each of these images has a size of 640 × 480 pixels. Singular points in the images are manually annotated and those lie close to fingerprint borders are not considered. Total 532 delta points and 966 core points are annotated in the database and are used for the performance analysis. A Poincare index algorithm proposed in [21] is used

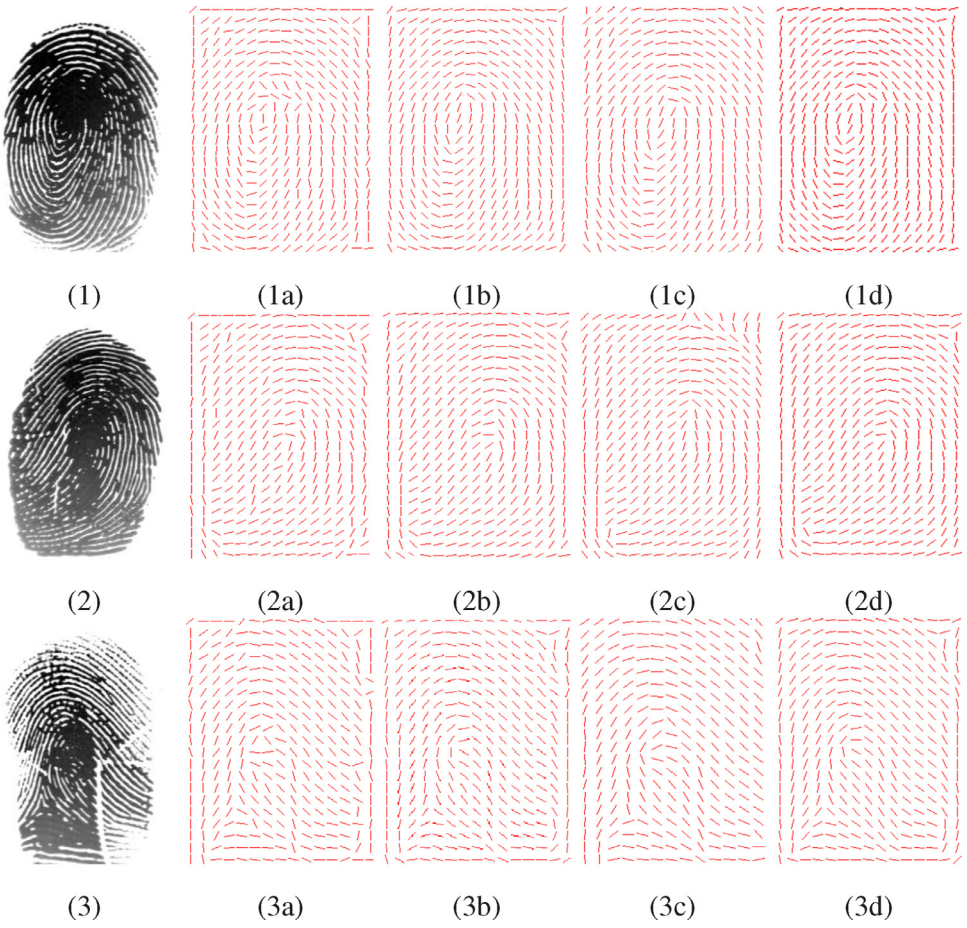

Fig. 3. Examples of OF modeling. Each row shows an example depicting following from left to right: (i) actual fingerprint, (ii) actual OF, (iii) modeled OF by the proposed regularization, (iv) modeled OF by only the weighted algorithm, (v) modeled OF by the proposed algorithm.

to extract the singular points. Performance in terms of singular point detection is determined using the following metrics:

$$\text{Precision} = \frac{\#\ True\ Positive}{\#\ True\ Positive + \#\ False\ Positive}, \tag{39}$$

$$\text{Recall} = \frac{\#\ True\ Positive}{\#\ True\ Positive + \#\ False\ Negative}, \tag{40}$$

$$\text{F-measure} = \frac{2 \times \text{Recall} \times \text{Precision}}{\text{Recall} + \text{Precision}}. \tag{41}$$

A singular point is considered to be a true positive if the Euclidean distance between its estimated location and annotated location is less than 24 pixels; otherwise it is considered as false positive. In addition, spurious detected singular points are considered as false positive, while undetected genuine singular points are considered as false negative. Therefore, higher values of Precision, Recall and F-measure indicate better singular point detection and localization, which in turn, indicate better OF modelling. On the other hand, average localization error is used to analyze the performance in terms of singular point localization. The Euclidean distance between the annotated and estimated location of a singular point gives the localization error of a singular point. Comparison between the proposed algorithm and various well known algorithms is shown in Table 1. In all these algorithms, OF estimated during preprocessing step is used for evaluation so as to maintain the consistency. In addition, four other algorithms denoted as *Algo I, Algo II, Algo III* and *Algo IV* are also studied for better analysis of the proposed algorithm. In *Algo I*, the proposed regularization is used but weighted OF modeling is not subsequently applied. It aims to understand the effectiveness of the proposed regularization. While in *Algo II, Algo III* and *Algo IV*, the proposed regularization is avoided and only the proposed weighted OF modeling is used such that weights are given

Table 1
Comparative Results of Singular Point Detection.

	Algorithm	*TP**	Precision+	Recall+	F-measure+	Error#
Delta	[15]	365	77.49	68.61	72.78	22.14
	[33]	368	80.88	69.17	74.57	20.68
	[34]	302	70.89	56.77	63.05	11.91
	[32]	372	80.69	69.92	74.92	20.82
	[22]	370	83.71	69.55	75.96	16.32
	Algo I	389	86.44	73.12	79.22	16.19
	Algo II	390	87.84	73.31	79.92	10.23
	Algo III	366	77.21	68.80	72.76	21.73
	Algo IV	376	85.26	70.68	77.29	10.56
	Proposed	*390*	*90.28*	*73.31*	*80.91*	*9.67*
Core	[15]	900	89.29	93.17	91.19	28.32
	[33]	918	91.16	95.03	93.05	25.61
	[34]	882	86.81	91.30	89.00	16.24
	[32]	913	90.76	94.51	92.60	25.89
	[22]	908	92.09	93.99	93.03	21.16
	Algo I	923	94.37	95.54	94.95	20.95
	Algo II	932	93.86	96.48	95.15	14.73
	Algo III	902	89.13	93.37	91.20	26.98
	Algo IV	919	93.58	95.13	94.35	15.47
	Proposed	*932*	*95.39*	*96.48*	*95.93*	*12.91*

* : # *True Positive*.
+ : Measured in %.
# : Average localization errors.

by the proposed weight estimation, foreground and background estimation proposed in [32] and probable location of singular points proposed in [34] respectively. These algorithms aim to understand the effectiveness of the proposed weight estimation and weighted OF modeling. Following observations can be derived from Table 1:

1. The difference among algorithms viz. *Algo II, Algo III, Algo IV*, [33] and [15] is the weight assignment. It can be observed that [15] has the lowest performance and as better weight assignments are used, performance increases. All the possible weight assignments proposed in the literature are covered in *Algo III, Algo IV*, algorithms proposed in [33] and [15]. Further, it can be seen that *Algo II* has better performance than *Algo III, Algo IV*, those presented in [33] and [15]. Thus, it can be inferred that the proposed weight estimation performs better than the existing weight estimation algorithms. Possible reasons for this are: (i) high weights are assigned to singular points close-by areas containing uniform flow that reduces the number of false negative and increases the number of true positives; and (ii) low weights are assigned in bad quality areas that enforces OF reconstruction in the bad quality areas and reduces the number of false positives.
2. The proposed regularization algorithm (*Algo I*) performs better than the algorithm in [22] because of better optimization algorithm and weight assignment. In contrast to the algorithm in [22], the proposed minimax formulation using data fidelity and regularization terms guarantees the global optimal or stable solution, i.e., better OF estimates. It reduces the number of spurious singular points (false negative) and increases the number of genuine singular points (true positive) that increases the Precision, Recall and F-measure. Similarly, weights are assigned in algorithm [22] using the saliency of singular points. It assigns low weights in linear flow areas and sometime assigns high weights in bad quality areas. Therefore, OF modeling using these weights allows preservation of spurious OF and reconstruction of genuine OF, which contradicts the aim of OF modeling. On the other hand, assignment of weights in *Algo I* enforces genuine OF preservation and spurious OF reconstruction during OF modeling.
3. It can be seen that *Algo II* has better singular point localization as compared to *Algo I*. Probable reason for this is that the estimated location a singular point is largely deviated from its actual location due to regularization in *Algo I*. This is usually the case when fingerprint contains large bad quality area near singular points. In such a scenario, local neighbors consist spurious OF estimates.
4. The proposed algorithm has better singular point detection and localization performance than *Algo I* or *Algo II*. It indicates that performance can be improved if both the regularization and weighted modeling are used for accurate OF estimation. For visualization, some examples of the proposed OF modeling are shown in Fig. 3.
5. Table 1 demonstrates that the proposed algorithm exhibit better performance than other well known algorithms.

3.3. OF deviation

In this section, the performance of the proposed algorithm is assessed using deviation of estimated OF from actual OF. Benchmark proposed in [53] has been used for the performance evaluation. It choses 60 poor quality fingerprint images from FVC2004 [51] and manually annotate the OF 1782 sparse locations. Manual annotations and the image names are available at [54]. Following performance metrics are used for assessment:

Table 2
Comparative Results of Singular Point Detection.

Algorithm	$Err_{\#}$	Err_{avg}
[15]	119	7.31
[33]	92	6.93
[34]	132	8.63
[32]	120	7.26
[22]	107	7.15
Algo I	87	6.35
Algo II	78	6.38
Algo III	113	7.27
Algo IV	85	6.89
Proposed	*69*	*5.84*

$*$: # *True Positive*. $^{+}$: Measured in %. $^{\#}$: Average localization errors.

1. If an OF estimated at a location differs from its actual OF by more than 15° then it is considered as spurious [53]. Total number of spurious estimates, $Err_{\#}$, is an indicator for the performance [53].
2. Consider a fingerprint image containing k annotated OF estimates represented as θ_A while $theta_B$ storing the corresponding modeled OF. Its OF deviation is given by:

$$e = \sqrt{\frac{\sum_{i=1}^{k} \left(\mathrm{F}\left(\theta_i^A, \theta_i^B\right)\right)^2}{k}}, \tag{42}$$

where function F is given by:

$$\mathrm{F}(\theta_1, \theta_2) = \begin{cases} \theta_1 - \theta_2 & if\ \frac{-\pi}{2} \le \theta_1 - \theta_2 < \frac{\pi}{2} \\ \pi + \theta_1 - \theta_2 & if\ \theta_1 - \theta_2 < \frac{-\pi}{2} \\ \pi - \theta_1 + \theta_2 & if\ \theta_1 - \theta_2 > \frac{\pi}{2}. \end{cases} \tag{43}$$

Average OF deviation, Err_{avg} for the database is used as another performance metric [27].

Lower values of $Err_{\#}$ and Err_{avg} indicate better performance. Comparisons of the proposed algorithm with various well known algorithms are shown in Table 2. Further, *Algo I* and *Algo II* are also used during comparison. Following observations are derived from Table 2:

1. Algorithm [33] is based on [15]. But it has used weighted modeling and has better OF modeling. Thus, it is observed that performance can be increased using appropriate weighted modeling. Another observation is that if high weights are assigned to areas requiring OF preservation and low weights are assigned in bad quality areas to enforce OF reconstruction, then modeled OF is found to be highly accurate and closely resembles the actual OF. The proposed weighted assignment fulfills these requirements and thus *Algo II* has better performance than [33] and [15]. Moreover, the proposed weight assignment performs better than *Algo III* and *Algo IV* which indicates that it is better than the weight assignments proposed in [32] and [34] respectively.
2. The proposed regularization algorithm (*Algo I*) performs better than the algorithm in [22] because of better optimization algorithm and weight assignment.
3. OF modeled by the proposed algorithm are more accurate than those modeled by *Algo I* or *Algo II*. It shows that it is better to use both the regularization and weighted modeling for OF modeling. In addition, Table 1 demonstrates that the proposed algorithm exhibit better performance than other well known algorithms.

3.4. Discussion

OF estimation using local methods gives spurious estimates in bad quality areas. Therefore, various regularization and global OF modeling based methods are subsequently applied for better estimates. Use of singular point detection and OF deviation show the better performance of the proposed algorithm. Regularization based OF modeling algorithms gives spurious estimates when local neighbors are insufficient to accurately estimate the OF, which is usually the case with fingerprints containing large bad quality area. In contrast, the weighted OF modelling based algorithm handles such cases but it can also model the noise due to over-fitting. If such noise is eliminated before applying weighted OF modeling then better performance can be expected. To leverage these intuitions, regularization followed by weighted OF modelling is used in the proposed algorithm. It has been experimentally shown that the performance can be improved if both regularization and weighted modeling are used for OF estimation.

4. Conclusions

There has been increasing demand of better fingerprint based recognition systems, especially the one that can handle the issues with bad quality fingerprints. Singular point detection, fingerprint image enhancement, fingerprint matching, fingerprint indexing, fingerprint synthesis, fingerprint registration and fingerprint classification are the key areas in designing such type of systems. Since OF is the prerequisite for these areas, an accurate OF estimation algorithm has been proposed in this paper. The proposed algorithm has commenced the use of both regularization and data-fitting algorithms for better OF modelling. It has used a novel OF regularization algorithm based on variational approach which has successfully preserved the genuine OF in the areas containing uniform flow and has accurately reconstructed the OF in bad quality areas. However, sometime it may generate spurious OF in singular points close-by areas. To get rid of this problem, weighted OF modelling based on Fourier basis has been subsequently applied. Experiments have been conducted on FVC2004DB1A. It is found that it is better to use both the regularization and weighted modeling for accurate OF estimation. Further, it has demonstrated that the proposed algorithm exhibits better performance that the other state of the art algorithms.

Acknowledgment

This work is partially supported by the Department of Information Technology (DIT), Government of India.

References

[1] B.J. Hill, An orientation field approach to modelling fibre-generated spatial point processes, University of Warwick, 2011 Ph.D. thesis.
[2] N.K. Ratha, S. Chen, A.K. Jain, Adaptive flow orientation-based feature extraction in fingerprint images, Pattern Recognit. 28 (11) (1995) 1657–1672.
[3] P. Gupta, P. Gupta, An efficient slap fingerprint segmentation and hand classification algorithm, Neurocomputing 142 (2014) 464–477, doi:10.1016/j.neucom.2014.03.049.
[4] P. Gupta, P. Gupta, Slap fingerprint segmentation using symmetric filters based quality, in: International Conference on Advances in Pattern Recognition, IEEE, 2015, pp. 1–6.
[5] P. Gupta, P. Gupta, Extraction of true palm-dorsa veins for human authentication, in: Indian Conference on Computer Vision Graphics and Image Processing, ACM, 2014, p. 35.
[6] P. Gupta, P. Gupta, Slap fingerprint segmentation, in: International Conference on Biometrics: Theory, Applications and Systems, IEEE, 2012, pp. 189–194.
[7] D. Maltoni, D. Maio, A.K. Jain, S. Prabhakar, Handbook of fingerprint recognition, Springer, 2009.
[8] L. Hong, Y. Wan, A. Jain, Fingerprint image enhancement: algorithm and performance evaluation, IEEE Trans. Pattern Anal. Mach. Intell. 20 (8) (1998) 777–789.
[9] J. Feng, J. Zhou, A.K. Jain, Orientation field estimation for latent fingerprint enhancement, IEEE Trans. Pattern Anal. Mach. Intell. 35 (4) (2013) 925–940.
[10] F. Alonso-Fernandez, J. Fierrez, J. Ortega-Garcia, J. Gonzalez-Rodriguez, H. Fronthaler, K. Kollreider, J. Bigun, A comparative study of fingerprint image-quality estimation methods, IEEE Trans. Inf. Forensics Secur. 2 (4) (2007) 734–743.
[11] X. Jiang, M. Liu, A.C. Kot, Reference point detection for fingerprint recognition, in: International Conference on Pattern Recognition, IEEE, 2004, pp. 540–543.
[12] B. Sherlock, D. Monro, A model for interpreting fingerprint topology, Pattern Recognit. 26 (7) (1993) 1047–1055.
[13] A.K. Jain, S. Prabhakar, L. Hong, S. Pankanti, Filterbank-based fingerprint matching, IEEE Trans. Image Process. 9 (5) (2000) 846–859.
[14] R. Cappelli, A. Lumini, D. Maio, D. Maltoni, Fingerprint image reconstruction from standard templates, IEEE Trans. Pattern Anal. Mach. Intell. 29 (9) (2007) 1489–1503.
[15] Y. Wang, J. Hu, D. Phillips, A fingerprint orientation model based on 2d fourier expansion (fomfe) and its application to singular-point detection and fingerprint indexing, IEEE Trans. Pattern Anal. Mach. Intell. 29 (4) (2007) 573–585.
[16] P. Gupta, P. Gupta, A robust singular point detection algorithm, Appl. Soft Comput. 29 (2015) 411–423.
[17] P. Gupta, P. Gupta, A dynamic slap fingerprint based verification system, in: International Conference on Intelligent Computing, Springer, 2014, pp. 812–818.
[18] A. Rao, R. Jain, Computerized flow field analysis: oriented texture fields, IEEE Trans. Pattern Anal. Mach. Intell. 14 (7) (1992) 693–709.
[19] K. Karu, A. Jain, Fingerprint classification, Pattern Recognit. 29 (3) (1996) 389–404.
[20] S. Chikkerur, A. Cartwright, V. Govindaraju, Fingerprint enhancement using stft analysis, Pattern Recognit. 40 (1) (2007) 198–211.
[21] A. Bazen, S. Gerez, Systematic methods for the computation of the directional fields and singular points of fingerprints, IEEE Trans. Pattern Anal. Mach. Intell. 24 (7) (2002) 905–919.
[22] Z. Hou, H.-K. Lam, W.-Y. Yau, Y. Wang, A variational formulation for fingerprint orientation modeling, Pattern Recognit. 45 (5) (2012) 1915–1926.
[23] S. Dass, Markov random field models for directional field and singularity extraction in fingerprint images, IEEE Trans. Image Process. 13 (10) (2004) 1358–1367.
[24] X. Yang, J. Feng, J. Zhou, Localized dictionaries based orientation field estimation for latent fingerprints, IEEE Trans. Pattern Anal. Mach. Intell. 36 (5) (2014) 955–969.
[25] S. Ram, H. Bischof, J. Birchbauer, Active fingerprint ridge orientation models, in: Advances in Biometrics, Springer, 2009, pp. 534–543.
[26] K. Lee, S. Prabhakar, Probabilistic orientation field estimation for fingerprint enhancement and verification, in: Biometrics Symposium, IEEE, 2008, pp. 41–46.
[27] F. Turroni, D. Maltoni, R. Cappelli, D. Maio, Improving fingerprint orientation extraction, IEEE Trans. Inf. Forensics Secur. 6 (3) (2011) 1002–1013.
[28] L. Fan, S. Wang, H. Wang, T. Guo, Singular points detection based on zero-pole model in fingerprint images, IEEE Trans. Pattern Anal. Mach. Intell. 30 (6) (2008) 929–940.
[29] N. Wu, J. Zhou, Model based algorithm for singular point detection from fingerprint images, in: International Conference on Image Processing, IEEE, 2004, pp. 885–888.
[30] J. Zhou, F. Chen, J. Gu, A novel algorithm for detecting singular points from fingerprint images, IEEE Trans. Pattern Anal. Mach. Intell. 31 (7) (2009) 1239–1250.
[31] J. Zhou, J. Gu, A model-based method for the computation of fingerprints' orientation field, IEEE Trans. Image Process. 13 (6) (2004) 821–835.
[32] S. Ram, H. Bischof, J. Birchbauer, Modelling fingerprint ridge orientation using legendre polynomials, Pattern Recognit. 43 (1) (2010) 342–357.
[33] X. Tao, X. Yang, K. Cao, R. Wang, P. Li, J. Tian, Estimation of fingerprint orientation field by weighted 2d fourier expansion model, in: International Conference on Pattern Recognition, IEEE, 2010, pp. 1253–1256.
[34] M. Liu, S. Liu, Q. Zhao, Fingerprint orientation field reconstruction by weighted discrete cosine transform, Inf. Sci. 268 (2014) 65–77.
[35] P. Gupta, P. Gupta, An accurate slap fingerprint based verification system, Neurocomputing (2015), doi:10.1016/j.neucom.2015.01.111.

[36] J. Bigun, T. Bigun, K. Nilsson, Recognition by symmetry derivatives and the generalized structure tensor, IEEE Trans. Pattern Anal. Mach. Intell. 26 (12) (2004) 1590–1605.
[37] H. Fronthaler, K. Kollreider, J. Bigun, J. Fierrez, F. Alonso-Fernandez, J. Ortega-Garcia, J. Gonzalez-Rodriguez, Fingerprint image-quality estimation and its application to multialgorithm verification, IEEE Trans. Inf. Forensics Secur. 3 (2) (2008) 331–338.
[38] P. Gupta, P. Gupta, Multi-modal fusion of palm-dorsa vein pattern for accurate personal authentication, Knowl. Based Syst. 81 (2015) 117–130.
[39] P. Gupta, P. Gupta, Fingerprint orientation modeling using symmetric filters, in: IEEE Winter Conference on Applications of Computer Vision, 2015.
[40] P. Gupta, P. Gupta, An accurate finger vein based verification system, Digit. Signal Process. 38 (2014) 43–52.
[41] B.N. Saha, N. Ray, Image thresholding by variational minimax optimization, Pattern Recognit. 42 (5) (2009) 843–856.
[42] A. Pascual-Iserte, D.P. Palomar, A.I. Pérez-Neira, M.Á. Lagunas, A robust maximin approach for MIMO communications with imperfect channel state information based on convex optimization, IEEE Trans. Signal Process. 54 (1) (2006) 346–360.
[43] G.W. Recktenwald, Finite-difference approximations to the heat equation, class notes, 2004, ⟨http://www.f.kth.se/~jjalap/numme/FDheat.pdf⟩.
[44] P. DuChateau, D. Zachmann, Applied partial differential equations, Courier Dover Publications, 2012.
[45] R. Thai, Fingerprint image enhancement and minutiae extraction, The university of western australia, 2003.
[46] Z.M. Kovacs-Vajna, R. Rovatti, M. Frazzoni, Fingerprint ridge distance computation methodologies, Pattern Recognit. 33 (1) (2000) 69–80.
[47] P.D. Kovesi, MATLAB and Octave functions for computer vision and image processing, Available from: ⟨http://www.csse.uwa.edu.au/~pk/research/matlabfns/⟩.
[48] K. Nilsson, J. Bigun, Localization of corresponding points in fingerprints by complex filtering, Pattern Recognit. Lett. 24 (13) (2003) 2135–2144.
[49] G. Evans, J. Blackledge, P. Yardley, Numerical methods for partial differential equations, Springer, Berlin, 2005.
[50] D.H. Bailey, Extra high speed matrix multiplication on the cray-2, SIAM J. Sci. Stat. Comput. 9 (3) (1988) 603–607.
[51] FVC2004, 2004, Available from: ⟨http://bias.csr.unibo.it/fvc2004/databases.asp⟩.
[52] D. Maio, D. Maltoni, R. Cappelli, J.L. Wayman, A.K. Jain, FVC2004: Third fingerprint verification competition, in: Biometric Authentication, Springer, 2004, pp. 1–7.
[53] C. Gottschlich, P. Mihailescu, A. Munk, Robust orientation field estimation and extrapolation using semilocal line sensors, IEEE Trans. Inf. Forensics Secur. 4 (4) (2009) 802–811.
[54] Annotated orientation field, Available from: ⟨http://www.stochastik.math.uni-goettingen.de/biometrics/⟩.